Available online at www.sciencedirect.com
ScienceDirect
Dyes and Pigments 77 (2008) 158–164
DYES and PIGMENTS
www.elsevier.com/locate/dyepig

Electrolytic treatment of C.I. Acid Orange 7 in aqueous solution using a three-dimensional electrode reactor

Lina Xu [a], Huazhang Zhao [a], Shaoyuan Shi [b], Guangzhi Zhang [a], Jinren Ni [a,*]

[a] Department of Environmental Engineering, Peking University, The Key Laboratory of Water and Sediment Sciences, Ministry of Education, Beijing 100871, China
[b] National Key Laboratory of Biochemical Engineering, Institute of Process Engineering, Chinese Academy of Sciences, Beijing 100080, China

Received 27 February 2007; received in revised form 23 April 2007; accepted 25 April 2007
Available online 6 May 2007

Abstract

A simulated wastewater containing the monoazo dye C.I. Acid Orange 7 was electrolytically treated using a three-dimensional electrode reactor equipped with granular activated carbon as particle electrode. The activated carbon fiber cathode was more effective than either a graphite or a stainless steel cathode due to its larger surface area which was beneficial to the electrogeneration of H_2O_2. Under the reaction conditions of 20 V and 3.0 g L^{-1} Na_2SO_4 at pH 3.0, decrease in the COD of up to 80%, and in the TOC by up to 72% were achieved and almost the complete decolorization of the dye was secured after 180 min electrolysis. Furthermore, decay of the dye followed a pseudo-first-order reaction in the first 60 min treatment. The three-dimensional electrode system generated more hydroxyl radicals than a two-dimensional system due to the formation of microelectrodes under applied high potential.

Keywords: Electrolytic treatment; Three-dimensional electrode reactor; Acid Orange 7; Activated carbon fiber; Degradation kinetics

1. Introduction

Since the first commercially available synthetic dye, Mauveine, was synthesized in 1875, dye industry has been playing an important role in daily life [1]. Global annual production of dye is estimated at $>7 \times 10^5$ tonnes, azo dyes, which are characterized by nitrogen-to-nitrogen double bonds (−N═N−), account for up to 70% of all textile dyes produced [2,3]. During manufacture or processing, ~15% of dyes is lost [4,5]. In China, $>1.6 \times 10^9$ m^3 of dye wastewater are generated annually [6], the disposal of which poses many problems [7,8]. In recent years, various physicochemical and biological methods, as well as a combination of the two, have been examined for the removal of dye molecules from wastewater [9–12]. However, as commercial dyes are intentionally designed to resist bio- and other degradation processes, each of the methods mentioned above suffer inherent disadvantages in terms of their applicability, efficiency or cost [13].

Recently, electrochemical oxidation process has attracted an increasing scientific and technical attention due to its high efficiency, ease of operation and environmental compatibility [14]. In essence, electrochemical processes involve the heterogeneous electron transfer between a solid electrode and the ionic species in an electrolytic solution [15]. Therefore, the rate of electrochemical reaction is dependent on electron transfer rate, which is directly proportional to the specific surface area of the electrode. However, enlarging the surface area cannot readily be achieved in a conventional two-dimensional electrode reactor.

The three-dimensional electrode was proposed in 1960s as a means of overcoming this problem [16]. In comparison to a two-dimensional electrode, many smaller particles are used in a three-dimensional electrode reactor. Under the influence of an electric field at an appropriate voltage, these particles

* Corresponding author. Tel.: +86 10 62751185; fax: +86 10 62756526.
E-mail address: nijinren@iee.pku.edu.cn (J. Ni).

0143-7208/$ - see front matter © 2007 Elsevier Ltd. All rights reserved.
doi:10.1016/j.dyepig.2007.04.004

can be polarized, forming charged microelectrodes, by means of which, the distance between the reactant and the electrode can be shortened thereby increasing, greatly, the specific surface area of the electrode, resulting in higher electrolytic efficiency.

Hitherto, the technology of three-dimensional electrode has been successfully applied to the electrosynthesis of organic compounds [17] and the removal of metal ions [18] or cyanide [19] from solution. In recent years, several papers have reported the application of this technology to eliminate organic pollutants, such as phenol [20], oxalates [18], chlorophenols [21] and human waste [22], from wastewater. In these investigations, stainless steel was usually used as the electrode. As several researchers demonstrated [15,23], besides direct anodic oxidation, the electrochemical degradation mechanism of organic pollutants in this particular electrode system is the electro-Fenton reaction, namely the indirect oxidation of H_2O_2 and hydroxyl radicals. Firstly, H_2O_2 and Fe^{2+} are electrogenerated at the cathode and anode, respectively (Eqs. (1) and (2)) [24,25].

$$O_2 + 2H^+ + 2e^- \rightarrow H_2O_2 (\text{on the cathode}) \quad (1)$$

$$Fe \rightarrow Fe^{2+} + 2e^- (\text{on the anode}) \quad (2)$$

Then, H_2O_2 diffuses into solution and reacts with the Fe^{2+} ions present in the solution, according to Fenton's reaction (Eq. (3)) [26]:

$$H_2O_2 + Fe^{2+} + H^+ \rightarrow Fe^{3+} + H_2O + OH^{\bullet} \quad (3)$$

The catalytic reaction (3) is propagated by Fe^{2+} regeneration, mainly by reduction of Fe^{3+} with H_2O_2 (Eq. (4)) [27].

$$Fe^{3+} + H_2O_2 \overset{H^+}{\leftrightarrow} [Fe - O_2H]^{2+} \leftrightarrow Fe^{2+} + HO_2^{\bullet} \quad (4)$$

Generally speaking, the previous studies of the three-dimensional electrode reactor focussed on the influence of operational parameters, such as voltage, electrolysis time, initial pH, etc., and little attention was paid to the influence of the electrode material, especially that of the cathode. As the cathode material plays an important role in the electro-Fenton reaction, it was decided to study the influence of different cathode materials on dye removal efficacy in the three-dimensional electrode system. In addition, this paper concerns the kinetics and the mechanism of dye degradation. C.I. Acid Orange 7 (AO7, Fig. 1) was chosen as a model azo dye because of its wide use in a variety of industries and stable characteristic with respect to biochemical oxidation [3,28].

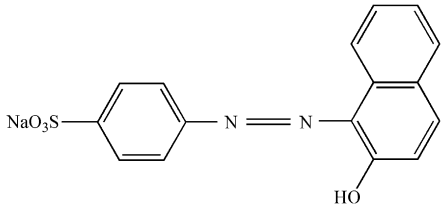

Fig. 1. Chemical structure of Acid Orange 7 (C.I. 15510).

2. Materials and methods

2.1. Materials

Granular activated carbon (GAC, model: KC-40) with a specific surface area of 910.68 $m^2\,g^{-1}$ and an average pore diameter of 2.10 nm was purchased from Beijing Kecheng Guanghua Activated Carbon Co., Ltd. (China) and used as particle electrodes in the study. The dye was supplied by Taixue Dyestuff Chemical Co., Ltd (China) and was used without further purification. All other chemicals used were of analytical reagent grade if not otherwise mentioned.

Deionized distilled water was used throughout this study. The initial dye concentration in the simulated wastewater was 300 mg L^{-1}. Anhydrous sodium sulfate was added as support electrolyte at a concentration of 3.0 g L^{-1}. The initial pH of the solution was adjusted to 3.0 by addition of 1 M aq H_2SO_4 to achieve optimal conditions for the electro-Fenton reaction [27].

A stainless steel plate (Beijing Zicheng Stainless Steel Products Co., Ltd., China) was used as anode; three electrode materials, namely activated carbon fiber (ACF) (Beijing Pacific Activated Carbon Products Co., Ltd, China), graphite (Beijing Sanye Carbon Co., Ltd, China) and stainless steel, were used as cathode. The physical properties of ACF and graphite are listed in Table 1.

2.2. Apparatus and procedure

Electrolysis was conducted in an undivided 1.0 dm^3 volume cylindrical glass tank (Fig. 2). A microporous plate attached to the lower part of the tank was used to support the particle electrode and disperse bubbles that arose form the compressed airy. Both anode and cathode were 7 cm × 5 cm in size and were situated 3 cm from each other. GAC (50.0 g) was packed between the cathode and anode to form a three-dimensional electrode.

Batch experiments were employed in this study as previously reported [21] to preclude dye removal due to its adsorption on GAC. Each batch of GAC could be used for 10 cycles under the same experimental conditions and each cycle lasted for 60 min. In the electrolysis process, if not otherwise mentioned, compressed air was sparged at a flow rate of 3.0 L min^{-1} and the three-dimensional electrode system was supplied with a constant voltage of 20 V DC. Aliquots were taken from the reactor at regular intervals and then centrifuged at 10,000 rpm using a TGL-16C centrifuge (Shanghai Anting Scientific Instrument Co., Ltd, China) for 10 min before further analysis.

Table 1
Primary physical properties of ACF and graphite

Sample	Thickness (mm)	Surface area ($m^2\,g^{-1}$)	Average pore diameter (nm)
ACF	3	764.13	1.92
Graphite	5	0.93	21.37

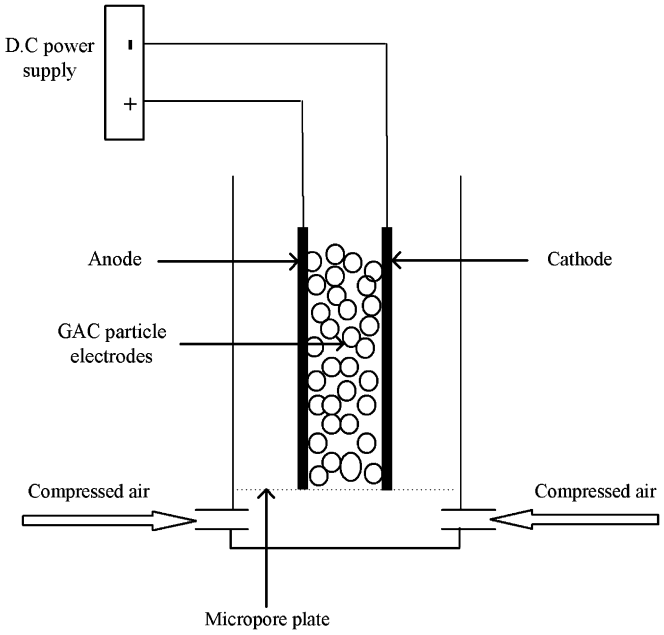

Fig. 2. Schematic diagram of the three-dimensional electrode reactor.

2.3. Analytical methods

Gas chromatography–mass spectrometry (GC–MS) was used for organic compounds analysis. Prior to GC–MS determination, a 300 mL sample was extracted using 10 mL CH_2Cl_2 (chromatogram pure grade, Fisher, USA) three times under acidic, neutral and alkaline conditions, respectively. The three extracted layers were mixed, dehydrated with anhydrous sodium sulfate and dried under nitrogen. The residue was dissolved in 1.0 mL CH_2Cl_2 and 1 μL was injected into a 6890N/5973 GC–MS system (Agilent, USA) equipped with a DB-35MS capillary column of inner diameter 0.25 mm and 30.0 m in length. The GC column was operated in temperature programmed mode at 40 °C for 5 min, increasing to 290 °C at an increment of 5 °C min^{-1} and finally holding at 290 °C for 10 min. Electron impact (EI) mode at 70 eV was used and the mass range scanned was 0–550 *m/z*. Analysis was undertaken with reference to the NIST02 mass spectral library database.

Hydroxyl radicals generated in the electrolysis process were trapped with dimethyl sulfoxide (DMSO) and quantified by HPLC [29]. DMSO (250 mM; chromatogram pure grade, Beijing Chemical Reagent Corporation, China) was used to generate formaldehyde quantitatively, which reacted with 2,4-dinitrophenylhydrazine (DNPH) to form the corresponding hydrazone (HCHO-DNPH) that was analyzed using an Agilent 1100 LC equipped with an Agilent Zorbax® SB-C18 column (150 × 4.6 mm, particle size 5 μm) and VWD detector set at 355 nm. The system had an injection loop of 20 μL and isocratic elution was carried out at a flow rate of 1.0 mL min^{-1}, using a mixture of methanol and water (60:40, v/v) as mobile phase.

Hydrogen peroxide concentration was determined spectrophotometrically using the iodide method [30]. A RuO_2/Ti mesh was used as anode in this experiment instead of stainless steel, with the purpose of eliminating the influence of Fenton reaction between Fe^{2+} and H_2O_2 especially at pH 3. Aliquots (6.0 mL) of the sample were mixed with 3.0 mL of 0.1 M potassium biphthalate and 3.0 mL of iodide reagent (0.4 M potassium iodide, 0.06 M NaOH, $\approx 10^{-4}$ M ammonium molybdate). The absorbance of the mixed solution was measured at 352 nm using a Specord 200 UV–vis spectrophotometer (Analytik Jena AG, Germany).

The UV–vis absorption spectrum of the dye was carried out in 10 mm quartz cuvettes; the UV–vis spectra were recorded from 190 to 800 nm using deionized water as blank. The decolorization rate of the dye was also measured using UV–vis spectrophotometry: from the absorbance of the samples at 484 nm, the λ_{max} of AO7, the decolorization rate was calculated according to Ref. [9]. The total organic carbon (TOC) and chemical oxygen demand (COD) of the samples were determined using a Multi N/C 3000 TOC analyser (Analytik Jena AG, Germany) and COD analyser (Hach, USA), respectively. pH was measured using a pH-201 meter (Hanna, Italy). The specific surface area and pore analysis of the electrode materials were measured by N_2 adsorption using a Micromeritics ASAP 2010.

3. Results and discussion

3.1. Dye degradation using different cathodes

Electrolysis was performed in the three-dimensional electrode reactor using ACF, graphite and stainless steel cathodes. As can be seen from Fig. 3, an increase of run number (N) particularly the first five runs, was accompanied by a decrease in the TOC removal by the three cathodes. Virgin GAC with high adsorption capacity was used as particle electrode in the experiments. The decrease of TOC in the first five runs shows the significant effect of dye adsorption on the GAC. However, the rate of decrease in TOC reduced with increasing run number as the GAC reached a saturation adsorption state.

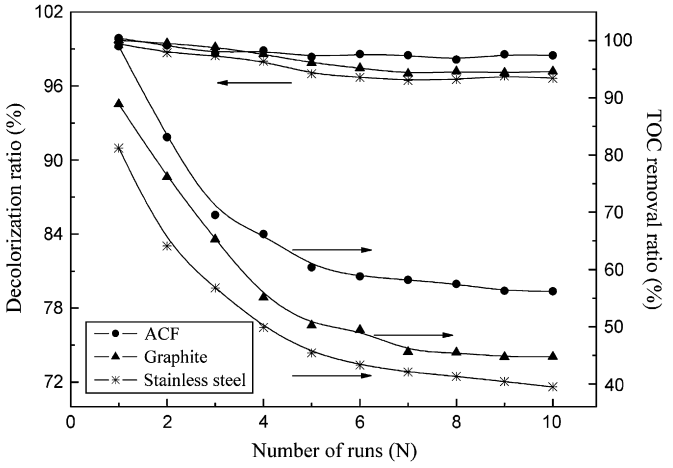

Fig. 3. Effect of cathode material on the removal ratio of color and TOC. Experimental conditions: the treatment time of each run: 60 min, pH: 3.0.

From the sixth run, TOC removal was at a constant level with relative standard deviation (RSD) < 5%. Similar trends in dye decolorization were observed. For the above-mentioned reasons, the latter five runs were adopted in the evaluation of the different cathodes, which made the analysis more focussed on the electrochemical effects of the electrodes rather than the dye adsorptive effects on the GAC. According to Fig. 3, it is apparent that the three cathode materials had high decolorisation ability; >96% decolorisation efficiency was achieved using the three electrodes and no apparent difference was observed between them. However, in the case of TOC removal, the difference between the electrodes was more evident. After 60 min electrolysis, the average TOC removal efficiency of ACF was ~57.4%, this being higher than that of graphite (46.0%) and stainless steel (41.3%). Although TOC removal could be used to evaluate the mineralization ability of the different cathode, the power consumption for reduction per unit TOC (in kWh kg^{-1}) was considered to be a better index. Based on the experimental results, the power consumption for ACF, graphite and stainless steel cathode system was 865, 1157, 1267 kWh kg^{-1} TOC, respectively, from which ACF showed the highest mineralization ability. As the electrogeneration of H_2O_2 at the cathode is related to the mineralization ability of the three-dimensional electrode system [30], the concentration of H_2O_2 was measured.

3.2. Electrogeneration of hydrogen peroxide using the different cathodes

The investigation of H_2O_2 generation was carried out using a two-dimensional electrode reactor, in which GAC was absent from the cell, so as to eliminate the adsorptive effect of GAC. The effect of charge on H_2O_2 generation is shown in Fig. 4; H_2O_2 generation increased with increasing applied charge. However, the generative velocity of H_2O_2 became much slower in the process due to the decomposition of H_2O_2 to O_2, or the oxidation of H_2O_2 to HO_2•[31]. Comparing the three lines in Fig. 4, it is evident that there was a distinct difference in H_2O_2 generation between ACF and the other two cathodes. When 5300 C of charge was supplied, ~170.94 μM H_2O_2 was electrogenerated by ACF compared to only 12.01 and 2.64 μM H_2O_2 produced by the graphite and stainless steel cathodes, respectively. Both the ACF and graphite cathodes were made from carbon, which is widely used for H_2O_2 generation due to its electrochemical activity towards oxygen reduction and its high overpotential for hydrogen evolution [32]. Compared with graphite, ACF showed better performance in H_2O_2 generation by virtue of its larger specific surface area (Table 1) and thus ACF was chosen as the most appropriate cathode for subsequent experiments. The finding that H_2O_2 generation was lower than that reported [30,33] may be due to different electrolysis conditions having been used. The high voltage (20 V) applied in electrolysis might induce side reactions of H_2O generation at the cathode (Eq. (5)) [33,34], and thus reduce the production of H_2O_2:

$$H_2O_2 + 2H^+ + 2e^- \rightarrow 2H_2O \quad (5)$$

3.3. Kinetic analysis of dye degradation

The GAC which had undergone 10 cycles was chosen as the particle electrode in order to avoid the negative influence of dye adsorption on GAC. The rate of dye degradation as a function of electrolysis time is given in Fig. 5. After 180 min, ~79.3% of COD and 71.9% of TOC reduction were achieved as well as almost complete dye decolorization (99.3%). The results fitted a pseudo-first-order reaction well in the first 60 min of electrolysis; the kinetic equations and parameters are shown in Table 2 from which it can be seen that the kinetic constant of dye degradation was apparently greater

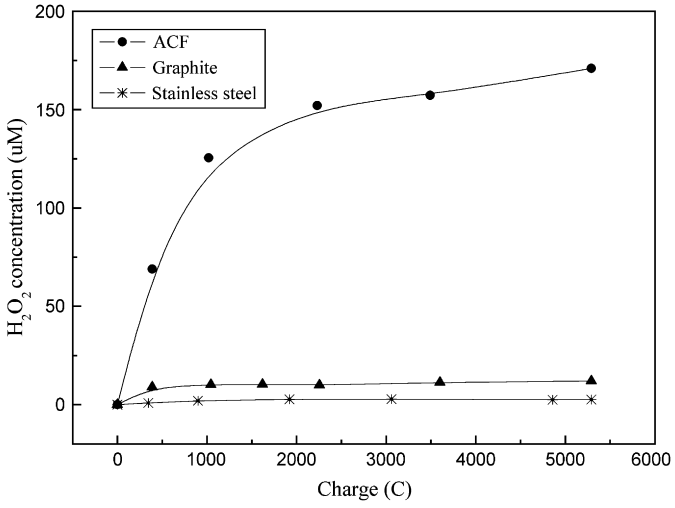

Fig. 4. Effect of charge on H_2O_2 concentration electrogenerated with different cathodes. Experimental conditions: 500 mL deionized water with 3 g L^{-1} Na_2SO_4 as the electrolyte, pH: 3.0.

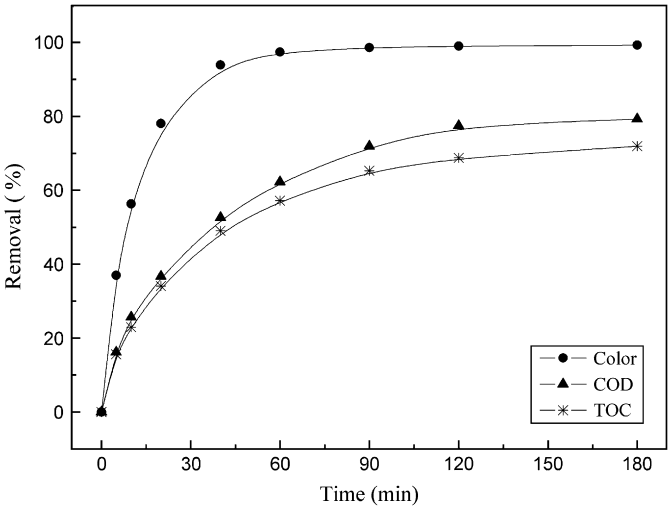

Fig. 5. Time-course of AO7 degradation in the three-dimensional electrode reactor with ACF as cathode. Experimental conditions: 500 mL of 300 mg L^{-1} AO7 solution with 3 g L^{-1} Na_2SO_4 as the electrolyte, pH: 3.0.

Table 2
Kinetic equations and parameters of AO7 degradation

Index	Kinetic equations	Regression coefficiency	Kinetic constant (min^{-1})	Half-life (min)
Color	$-\ln(color_t) = 0.0592t + 0.095$	0.9932	0.0592	11.71
COD	$-\ln(COD_t) = 0.0148t - 5.523$	0.9895	0.0148	46.83
TOC	$-\ln(TOC_t) = 0.013t - 2.6989$	0.9816	0.013	53.32

than that of COD or TOC reduction, suggesting that the dye was oxidized first to colourless intermediates and then to CO_2.

3.4. UV–vis spectral changes

The UV–vis spectra of AO7 from 190 to 800 nm are shown in Fig. 6. It can be seen that the absorption spectrum at pH 3.0 was characterized by a maximum peak at 484 nm and two peaks at 229 and 311 nm. The peak in the visible region can be attributed to the n–π* transition of the azo group while those at 229 and 311 nm are due to the π–π* transition of the benzene and naphthalene rings, respectively, bonded to the azo in the dye molecule [4,35]. Fig. 6 reveals that all of the adsorption peaks were weakened, indicating that the relevant structures were destroyed. In order to compare the degradative velocity of the three main structures mentioned above, the normalized intensities of the absorption peaks of the benzene ring located at 229 nm, the naphthalene ring at 311 nm and the azo group at 484 nm were plotted as functions of electrolysis time in Fig. 7. It was observed that the intensity of the peak at 484 nm decreased much faster than those of the other two peaks. The slower decrease of the intensities of the two UV peaks may be attributed to the formation of intermediates, resulting from the degradation of AO7 in the three-dimensional electrode system, which still contain benzoic- and naphthalene-type rings [4].

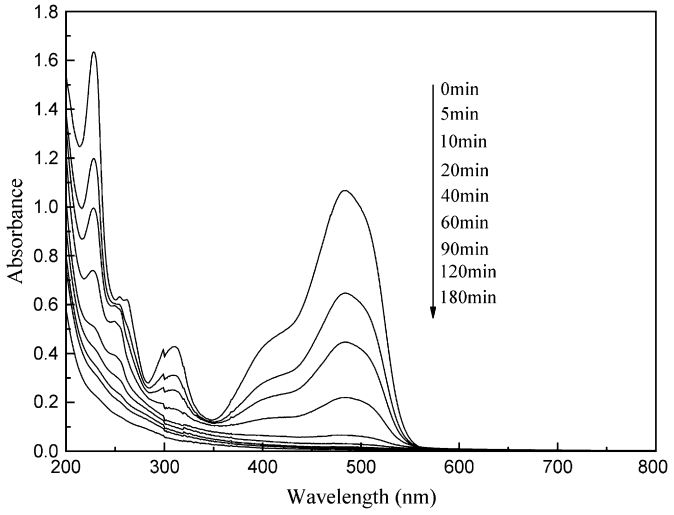

Fig. 6. UV–vis spectral change of AO7 with different electrolysis time. Experimental conditions: as shown in Fig. 5.

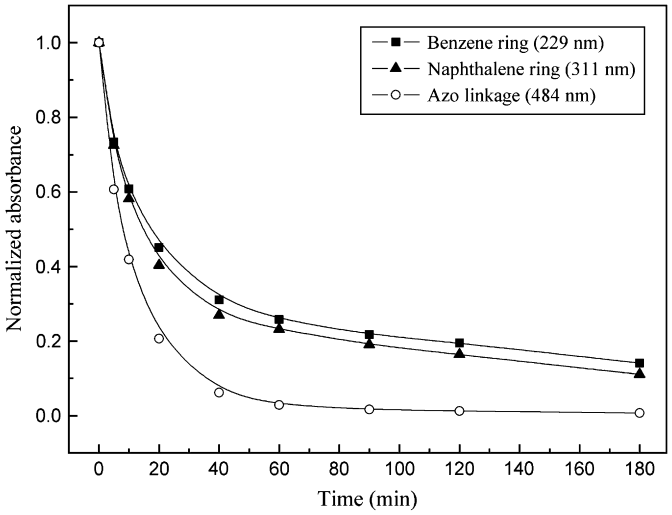

Fig. 7. Normalized absorbance of the three main UV–vis absorbance bands of AO7 vs electrolysis time. Experimental conditions: as shown in Fig. 5.

3.5. Generation of hydroxyl radicals

Hydroxyl radical, a reactive oxidant with the potential of 2.80 V [36], plays an important role in the degradation of organic compounds in electrochemical systems [37]. Due to its high activity, low concentration and short lifetime, there is no direct method to prove its existence and, therefore, spin traps are commonly used for its indirect measurement [38,39]. In this context, DMSO is conveniently used to trap hydroxyl radicals and linearity is observed between the concentration of hydroxyl radicals and the peak area of the DNPH–HCHO derivatives in the HPLC chromatogram [29].

The quantification of hydroxyl radicals generated in both the three-dimensional and the two-dimensional electrode reactors are shown in Fig. 8; differences in hydroxyl radical generation occurred in these two systems. After ~4500 C of

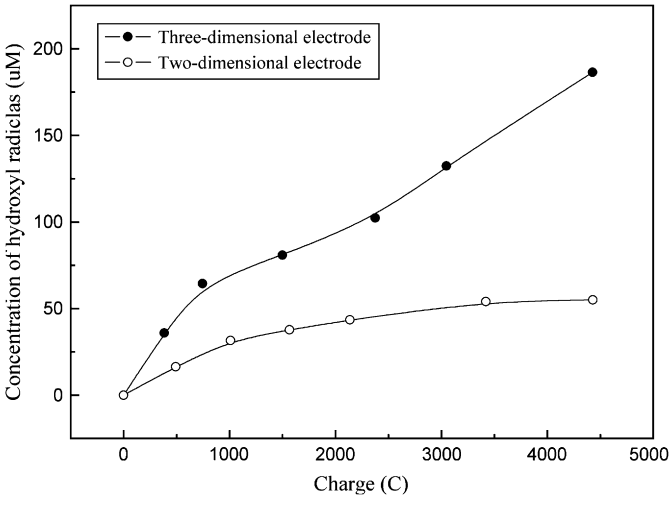

Fig. 8. Generation of hydroxyl radicals in two-dimensional and three-dimensional electrode system. Experimental conditions: 250 mM DMSO solution with 3 g L^{-1} Na_2SO_4 as the electrolyte, ACF adopted as cathode, pH: 3.0.

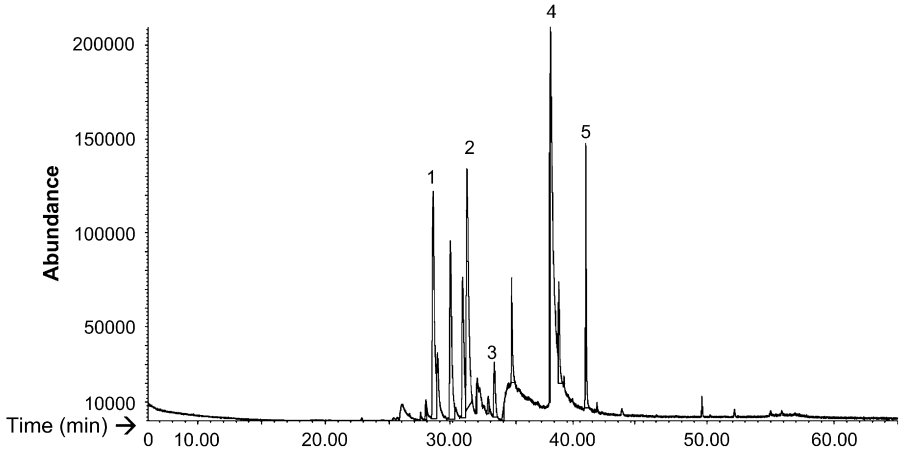

Fig. 9. GC–MS chromatograms of samples after electrochemical treatment in three-dimensional electrode reactor. Experimental conditions: as shown in Fig. 5. (1) Butanedioic acid, bis(2-methylpropyl) ester, (2) 2*H*-1-benzopyran-2-one, (3) hexanedioic acid, bis(2-methylpropyl) ester, (4) 1,2-dihydroxynaphthalene, and (5) 1,2-benzenedicarboxylic acid, butyl 2-methylpropyl ester.

charge was supplied, the concentration of radicals generated in the two-dimensional system was ~50 μM compared to ~190 μM, in the three-dimensional system, this being nearly four times that of the former. If the negative influence of GAC adsorption on the hydroxyl radicals is considered, the difference between these two systems is more evident. As hydroxyl radicals in these systems were mainly generated through the electro-Fenton reaction, the result shown in Fig. 8 may be due to the formation of many microelectrodes via polarization of the GAC under the applied high potential. This observation confirms the electrolytic principle of the three-dimensional electrode reactor [40].

3.6. GC–MS analysis

GC–MS analysis was performed to identify the intermediate products formed in the liquid phase during the electrochemical treatment of the dye in the three-dimensional electrode reactor. After 60 min electrolytic treatment, the dominant organic compounds detected were aromatic hydrocarbon and ester substances (Fig. 9). Although all the identified compounds were not the degradation products of AO7, the result confirms the cleavage of the benzene and naphthalene rings as a result of electrolysis. Zhang et al. [41] reported that under oxidation conditions, AO7 was first decomposed to aromatic intermediates and further oxidized to ring-opened products, which were then finally mineralized to CO_2, H_2O and inorganic salts. However, the degradation mechanism of AO7 may differ depending on the different treatment methods used [3,41]. Thus more work is needed on intermediate product analysis so as to reveal the precise degradation mechanism of AO7 in the three-dimensional electrode reactor.

4. Conclusions

Whilst all three cathodes showed high efficiency in the decolorization of AO7 (>96% after 60 min of electrolysis), the TOC removal of ACF (57.4%) was much higher than that of graphite (46.0%) or stainless steel (41.3%). Furthermore, the power consumption of the ACF cathode system was 865 kWh kg^{-1} TOC, which was smaller than the 1157 kWh kg^{-1} TOC of the graphite system and the 1267 kWh kg^{-1} TOC of the stainless steel system. These findings can be attributed to the fact that ACF was more suitable for H_2O_2 generation due to its large specific surface area. Dye degradations conformed to pseudo-first-order kinetics and the kinetic constant of dye degradation was greater than that of COD or TOC removal. It is proposed that more hydroxyl radicals were generated in the three-dimensional electrode system than in the two-dimensional system, because of the formation of many microelectrodes in the three-dimensional electrode system under the applied high potential. Some aromatic hydrocarbon and ester compounds were observed from the electrolysis process using GC–MS, indicating cleavage of the benzene and naphthalene rings in the dye had occurred.

Acknowledgements

The authors are grateful to the National Nature Science Foundation of China for financial support with Grant no. 20607001.

References

[1] Cao JS, Wei LP, Huang QG, Wang LS, Han SK. Reducing degradation of azo dye by zero-valent iron in aqueous solution. Chemosphere 1999;38(3):565–71.
[2] Xu XR, Li HB, Wang WH, Gu JD. Degradation of dyes in aqueous solutions by the Fenton process. Chemosphere 2004;57(7):595–600.
[3] Rismayani S, Fukushima M, Ichikawa H, Tatsumi K. Decolorization of orange-II by catalytic oxidation using iron(III) phthalocyanine-tetrasulfonic acid. J Hazard Mater 2004;114(1–3):175–81.
[4] Stylidi M, Kondarides DI, Verykios XE. Pathways of solar light-induced photocatalytic degradation of azo dyes in aqueous TiO_2 suspensions. Appl Catal B: Environ 2003;40(4):271–86.
[5] Bauer C, Jacques P, Kalt A. Photooxidation of an azo dye induced by visible light incident on the surface of TiO_2. J Photochem Photobiol A 2001;140(1):87–92.

[6] Liu G, Wu T, Zhao J, Hidaka H, Serpone N. Photoassisted degradation of dye pollutants. 8. Irreversible degradation of alizarin red under visible light radiation in air-equilibrated aqueous TiO2 dispersions. Environ Sci Technol 1999;33:2081–7.
[7] Van der Zee FP, Bisschops IAE, Lettinga G, Field JA. Activated carbon as an electron acceptor and redox mediator during the anaerobic biotransformation of azo dyes. Environ Sci Technol 2003;37(2):402–8.
[8] Vinodgopal K, Wynkoop DE, Kamat PV. Environmental photochemistry on semiconductor surfaces: photosensitized degradation of a textile azo dye, acid orange 7, on TiO_2 particles using visible light. Environ Sci Technol 1996;30(5):1660–6.
[9] Coughlin MF, Kinkle BK, Bishop PL. Degradation of acid orange 7 in an aerobic biofilm. Chemosphere 2002;46(1):11–9.
[10] Wu TX, Lin T, Zhao JC, Hidaka H, Serpone N. TiO_2-assisted photodegradation of dyes. 9. Photooxidation of a squarylium cyanine dye in aqueous dispersions under visible light irradiation. Environ Sci Technol 1999;33(9):1379–87.
[11] Ghoreishi SM, Haghighi R. Chemical catalytic reaction and biological oxidation for treatment of non-biodegradable textile effluent. Chem Eng J 2003;95:163–9.
[12] Shu HY, Huang CR, Chang MC. Decolorization of mono-azo dyes in waste-water by advanced oxidation process—a case-study of Acid-Red-1 and Acid-Yellow-23. Chemosphere 1994;29(12):2597–607.
[13] Chu W, Ma C-W. Quantitative prediction of direct and indirect dye ozonation kinetics. Water Res 2000;34(12):3153–60.
[14] Chiang LC, Chang JE, Tseng SC. Electrochemical oxidation pretreatment of refractory organic pollutants. Water Sci Technol 1997;36 (2–3):123–30.
[15] Fockedey E, Van Lierde A. Coupling of anodic and cathodic reactions for phenol electro-oxidation using three-dimensional electrodes. Water Res 2002;36(16):4169–75.
[16] Backhurst JR, Coulson JM, Goodridge F, Plimley RE. A preliminary investigation of fluidized bed electrodes. J Electrochem Soc 1969;116(11):1600–7.
[17] Dieckmann GR, Langer SH. Selective electrogenerative oxidation of benzyl alcohol with platinum-graphite packed-bed anodes. J Appl Electrochem 1997;27:1–8.
[18] Xiong Y, Karlsson HT. An experimental investigation of chemical oxygen demand removal from the wastewater containing oxalic acid using three-phase three-dimensional electrode reactor. Adv Environ Res 2002;7(1):139–45.
[19] El-Ghaoui EA, Jansson REW, Moreland C. Application of the trickle tower to problems of pollution control. II. The direct and indirect oxidation of cyanide. J Appl Electrochem 1982;12(1):69–73.
[20] Xiong Y, He C, Karlsson HT, Zhu XH. Performance of three-phase three-dimensional electrode reactor for the reduction of COD in simulated wastewater-containing phenol. Chemosphere 2003;50(1):131–6.
[21] Polcaro AM, Palmas S, Renoldi F, Mascia M. Three-dimensional electrodes for the electrochemical combustion of organic pollutants. Electrochim Acta 2000;46:389–94.
[22] Tennakoon CLK, Bhardwaj RC, Bockris JO. Electrochemical treatment of human wastes in a packed bed reactor. J Appl Electrochem 1996;26(1):18–29.
[23] An TC, Zhu XH, Xiong Y. Feasibility study of photoelectrochemical degradation of methylene blue with three-dimensional electrode-photocatalytic reactor. Chemosphere 2002;46(6):897–903.
[24] Boye B, Dieng MM, Brillas E. Degradation of herbicide 4-chlorophenoxyacetic acid by advanced electrochemical oxidation methods. Environ Sci Technol 2002;36(13):3030–5.
[25] Oturan MA, Peiroten J, Chartrin P, Acher AJ. Complete destruction of *p*-nitrophenol in aqueous medium by electro-Fenton method. Environ Sci Technol 2000;34(16):3474–9.
[26] Neyens E, Baeyens J. A review of classic Fenton's peroxidation as an advanced oxidation technique. J Hazard Mater 2003;98:33–50.
[27] Brillas E, Boye B, Sires I, Garrido JA, Rodriguez RM, Arias C, et al. Electrochemical destruction of chlorophenoxy herbicides by anodic oxidation and electro-Fenton using a boron-doped diamond electrode. Electrochim Acta 2004;49(25):4487–96.
[28] Fernandes A, Morao A, Magrinho M, Lopes A, Goncalves I. Electrochemical degradation of C.I. Acid Orange 7. Dyes Pigments 2004;61(3):287–96.
[29] Tai C, Peng JF, Liu JF, Jiang GB, Zou H. Determination of hydroxyl radicals in advanced oxidation processes with dimethyl sulfoxide trapping and liquid chromatography. Anal Chim Acta 2004;527(1):73–80.
[30] Wang AM, Qu JH, Ru J, Liu HJ, Ge JT. Mineralization of an azo dye Acid Red 14 by electro-Fenton's reagent using an activated carbon fiber cathode. Dyes Pigments 2005;65(3):227–33.
[31] Harrington T, Plecher D. The removal of low levels of organics from aqueous solutions using Fe(II) and hydrogen peroxide formed in situ at gas diffusion electrodes. J Electrochem Soc 1999;146(8):2983–9.
[32] Panizza M, Cerisola G. Removal of organic pollutants from industrial wastewater by electrogenerated Fenton's reagent. Water Res 2001;35(16):3987–92.
[33] Qiang ZM, Chang JH, Huang CP. Electrochemical generation of hydrogen peroxide from dissolved oxygen in acidic solutions. Water Res 2002;36(1):85–94.
[34] Brillas E, Casado J. Aniline degradation by electro-Fenton and peroxi-coagulation processes using a flow reactor for wastewater treatment. Chemosphere 2002;47(3):241–8.
[35] Wu F, Deng NS, Hua HL. Degradation mechanism of azo dye C.I. reactive red 2 by iron powder reduction and photooxidation in aqueous solutions. Chemosphere 2000;41(8):1233–8.
[36] Legrini O, Oliveros E, Braun AM. Photochemical processes for water treatment. Chem Rev 1993;93(2):671–98.
[37] Feng JY, Hu XJ, Yue PL. Discoloration and mineralization of orange II using different heterogeneous catalysts containing Fe: a comparative study. Environ Sci Technol 2004;38(21):5773–8.
[38] Li YJ, Wang F, Zhou GD, Ni YM. Aniline degradation by electrocatalytic oxidation. Chemosphere 2003;53(10):1229–34.
[39] Comninellis C. Electrocatalysis in the electrochemical conversion/combustion of organic pollutants for waste water treatment. Electrochim Acta 1994;39(11–12):1857–62.
[40] Kong WP, Wang B, Ma HZ, Gu L. Electrochemical treatment of anionic surfactants in synthetic wastewater with three-dimensional electrodes. J Hazard Mater 2006;137(3):1532–7.
[41] Zhang SJ, Yu HQ, Li QR. Radiolytic degradation of Acid Orange 7: A mechanistic study. Chemosphere 2005;61(7):1003–11.